

Handling Non-ignorably Missing Features in Electronic Health Records Data Using Importance-Weighted Autoencoders

David K. Lim*

Department of Biostatistics, University of North Carolina at Chapel Hill
and

Naim U. Rashid

Department of Biostatistics, University of North Carolina at Chapel Hill
and

Junier B. Oliva

Department of Computer Science, University of North Carolina at Chapel Hill
and

Joseph G. Ibrahim

Department of Biostatistics, University of North Carolina at Chapel Hill

December 23, 2024

Abstract

Electronic Health Records (EHRs) are commonly used to investigate relationships between patient health information and outcomes. Deep learning methods are emerging as powerful tools to learn such relationships, given the characteristic high dimension and large sample size of EHR datasets. The Physionet 2012 Challenge involves an EHR dataset pertaining to 12,000 ICU patients, where researchers investigated

*The authors gratefully acknowledge NIH for funding this research.

the relationships between clinical measurements, and in-hospital mortality. However, the prevalence and complexity of missing data in the Physionet data present significant challenges for the application of deep learning methods, such as Variational Autoencoders (VAEs). Although a rich literature exists regarding the treatment of missing data in traditional statistical models, it is unclear how this extends to deep learning architectures. To address these issues, we propose a novel extension of VAEs called Importance-Weighted Autoencoders (IWAEs) to flexibly handle Missing Not At Random (MNAR) patterns in the Physionet data. Our proposed method models the missingness mechanism using an embedded neural network, eliminating the need to specify the exact form of the missingness mechanism *a priori*. We show that the use of our method leads to more realistic imputed values relative to the state-of-the-art, as well as significant differences in fitted downstream models for mortality.

Keywords: missing data, autoencoder, MNAR, EHR

1 Introduction

Electronic Health Records (EHRs) are a broad and popular class of data pertaining to records of patient information, including diagnostic measurements, laboratory results, and medical history (Zhang et al. 2020). Analysis of such data can be crucial for uncovering patterns that may be informative for patient care, such as associations between certain diagnostic measurements and mortality, (Courtright et al. 2019) and also represent an inexpensive means to recruit patients for clinical research (Beesley & Mukherjee 2020). EHR data from the Physionet Challenge (Silva et al. 2012), which called on participants to develop a model that best predicts Intensive Care Unit (ICU) mortality, based upon data pertaining to 12,000 patients admitted into the Beth Israel Deaconess Medical Center. Such models would allow for the early identification of ICU patients with an elevated risk of mortality based upon common clinical measurements, and would therefore have great utility for health practitioners.

The presence of high-dimensional and complex interactions among features in EHR data has motivated the use of deep learning methods for learning such relationships. For example, autoencoders (AE) are a popular class of deep learning architectures that has shown great utility across a range of applications in EHR data. Such applications include dimension reduction, representational learning, and the generation of synthetic data mimicking real EHR data, which may be unavailable due to patient confidentiality (Shickel et al. 2018, Sadati et al. 2019, Gootjes-Dreesbach et al. 2019). The structure of the AE consists of an encoder, which “encodes” the data into a lower-dimensional space that captures the salient qualities of the data, and a decoder, which reconstructs the original data from the lower-dimensional space (Tschannen et al. 2018). This lower dimensional space, similar to PCA, may be used to define structure in the underlying set of input data (Wang et al. 2016).

From this low dimensional space, the generator “reconstructs” the data, which allows it to also generate synthetic data that reflects the original data. The encoder and decoder are often represented by feed forward neural networks, allowing for complex non-linear interactions to be captured in both (LeCun et al. 2015). The Variational Autoencoder (VAE) is built upon the same encoder-decoder structure, but imposes a probabilistic assumption on the data, as well as the lower-dimensional (or “latent”) space (Doersch 2016), and uses variational inference to learn a tractable estimate of the posterior of the latent variable conditional on the observed data (Kingma & Welling 2013, Rezende et al. 2014). In prior evaluations, VAEs have shown tremendous performance in data generation and representation learning (van den Oord et al. 2017), which explain their popularity in EHR data and many other applications.

However, the Physionet data also contain a significant proportion of missing entries across measurements. In general, the common and widespread presence of missing data across patient records (Luo et al. 2018) presents a significant barrier to the generalizability and applicability of deep learning methods (Wells et al. 2013). EHR data also typically contain many features pertaining to a large number of patients (Ross et al. 2014), and such features may show complex interactions with each other as well as with clinical outcomes (Vinzamuri & Reddy 2013), compounding the impact of the missingness of these features. The conventional statistical literature characterizes patterns of missingness into one of three mechanisms: missing completely at random (MCAR), missing at random (MAR), or missing not at random (MNAR) (Little & Rubin 2002). Many methods submitted to the challenge utilized naïve methods such as zero or mean imputation (Citi & Barbieri 2012, Johnson et al. 2014) to replace missing values prior to model training, while others employed imputation methods that can handle MAR missingness, but not MNAR

(Fortuin et al. 2019). A limited number of existing VAE methods claim to allow MAR patterns of missingness among input features during training (Nazabal et al. 2018, Mattei & Frellsen 2019, Ivanov et al. 2019); however, a thorough evaluation of performance under the MCAR and MAR settings is lacking in the literature. In addition, missingness in EHR datasets is often not ignorable, i.e. MNAR (Beaulieu-Jones & and 2016, Venugopalan et al. 2019, Sharafoddini et al. 2019, O’Shea 2019), requiring principled and theoretically sound methods of handling missing data prior to or during model training. To the best of our knowledge, there are no published methods that can handle MNAR patterns of missingness in the VAE setting, and this presents a significant barrier to the application of such methods to EHR and other modern biomedical datasets.

To address these issues, we introduce a novel architecture that treats missing observations as latent variables using Importance-Weighted Autoencoders (IWAEs), incorporating the modeling of the missingness mechanism directly into the network structure and enabling our approach to handle MNAR missingness in input features for the first time. In contrast to traditional likelihood-based missing data methods, we do not need to pre-specify the set of features to model the probability of missingness. We instead model this probability with a feed forward neural network, facilitating the flexible handling of MNAR patterns of missingness across a large set of available features. Through simulations, we show that proper modelling of the missingness mechanism increases the accuracy of missing data imputation. Lastly, we show that in the Physionet 2012 Challenge EHR dataset, accounting for MNAR missingness results in more realistic ranges of imputed diagnostic measurements relative to those imputed using a MAR model, in addition to significant differences in downstream fitted models to predict in-hospital mortality. In addition, we believe that our work can be extended more generally to be a flexible framework to handle multiple patterns of

missingness in similar EHR and other complex biomedical datasets.

2 Data

The Physionet 2012 Challenge dataset (Silva et al. 2012) is a publicly available EHR dataset that consists of de-identified information on 12,000 adult Intensive Care Unit (ICU) patients admitted at Beth Israel Deconess Medical Center from 2001 and 2008. Patients whose ICU stays were less than 48 hours long were excluded from the dataset. For each patient, 36 features were measured, with one potential measurement hourly for 48 hours. Example features include albumin levels (in g/dL), serum sodium (in mEq/L) and white blood cell count (in cells/nL). For each patient, clinical outcomes such as the SAPS-I score (Gall et al. 1984) SOFA score (Ferreira 2001), length of stay, survival, and in-hospital death were also recorded. The challenge called for learning algorithms to accurately predict the outcome of interest (like in-hospital death) based on such clinical data, facilitating clinical decision-making regarding the need for early intervention in ICU patients (Silva et al. 2012).

The challenge dataset was divided into training, validation, and test datasets of equal sizes, and missingness was highly prevalent in all three datasets. Table 1 shows the missingness percentage of all features in the dataset, and the number of subjects with at least one non-missing entry recorded for each respective feature. In this study, we pre-processed the data using the same method as the top performing method of the Physionet 2012 Challenge, which used a priori knowledge of medical data to remove nonsensical values and condense the time-series data into summary statistics across the repeated measurements (Johnson et al. 2012). For our analysis, we used the median or last-observed measurements for each clinical measurement. In this way, an entry is missing only if the diagnostic mea-

sure was not taken during any of the 48 time points, as most measurements are not meant to be taken hourly. After the pre-processing, the dataset consisted of 46 features, including 7 baseline measurements. Additional details of this pre-processing step can be found in Section 1.2 of the Supplementary materials.

As shown in previous work, VAEs are natural architectures to utilize in this setting, as VAEs inherently learn a probabilistic model of the data, and samples from this model can be used to impute missing values. Such imputed values may be useful to perform downstream statistical analyses, such as prediction of mortality (Sharafoddini et al. 2019). However, some studies have suggested that such missingness in EHR data may be MNAR (Sharafoddini et al. 2019, O’Shea 2019), but existing VAE-based imputation methods can only handle MCAR or MAR missingness, and is unable to handle the more difficult MNAR mechanisms that may be present in this type of data. A model that accounts for such non-ignorable, or MNAR, missingness may most accurately impute missing values in the Physionet 2012 Challenge dataset, and allow for accurate analysis of the patient data.

3 Methods

In this section, we first show the formulation of the VAE and its generalization (IWAE) in Section 3.1. Then, in Section 3.2 we review the different mechanisms of missingness in the context of the historical statistical literature (Little & Rubin 2002). We expand on the case of MNAR, or non-ignorable missingness, and present the models that are typically employed under this type of missingness. In Section 3.3, we introduce a novel method using the IWAE architecture in the presence of MNAR missingness.

3.1 Variational Autoencoder

A variational autoencoder (VAE) is a type of deep learning architecture in which the input data is autoencoded using a stochastic encoder-decoder pair to optimize an objective function that encourages the encoded latent space to follow an assumed fixed prior distribution (Ghosh et al. 2019). Let \mathbf{X} be the $n \times p$ data matrix with observation vectors \mathbf{x}_i for observations $i = 1, \dots, n$, with corresponding entries x_{ij} denoting values of the features $j = 1, \dots, p$ for each observation. In a VAE, we assume observation vectors \mathbf{x}_i are i.i.d. samples generated from an unknown underlying process $p_\psi(\cdot|z)$ involving a latent variable \mathbf{Z} from some prior distribution $p(\mathbf{Z})$ (Kingma & Welling 2019), where \mathbf{Z} is an $n \times d$ matrix, such that $\mathbf{Z} = \{\mathbf{z}_1, \dots, \mathbf{z}_n\}$ with \mathbf{z}_i latent vectors of length d for each observation $i = 1, \dots, n$.

Learning is done by maximizing an objective function via variational inference (Blei et al. 2016). Ideally, we wish to maximize the marginal log-likelihood of \mathbf{X} , defined as $\log p_\psi(\mathbf{X}) = \log \int p_\psi(\mathbf{X}, \mathbf{Z}) d\mathbf{Z}$, for some set of parameters ψ . However, due to the integral involved, this quantity is usually intractable. Thus, instead of directly maximizing the marginal log-likelihood, we utilize variational inference, which aims to maximize the so-called ‘‘Evidence Lower Bound’’ (ELBO). The standard ELBO gives a lower bound of the marginal log-likelihood and has the form:

$$\mathcal{L}(\theta, \psi) = \mathbb{E}_{\mathbf{Z} \sim q_\theta(\mathbf{Z}|\mathbf{X})} \log \left[\frac{p_\psi(\mathbf{X}|\mathbf{Z})p(\mathbf{Z})}{q_\theta(\mathbf{Z}|\mathbf{X})} \right], \quad (1)$$

where $\mathcal{L}(\theta, \psi)$ is the ELBO such that $\log p(\mathbf{X}) \geq \mathcal{L}(\theta, \psi)$, $p(\mathbf{Z})$ is the prior distribution of \mathbf{Z} , p_ψ is a multivariate ‘‘generative model’’ conditional on \mathbf{Z} , and q_θ is a multivariate ‘‘recognition model’’ conditional on \mathbf{X} . Furthermore, we denote $f_\psi(\mathbf{Z})$ and $g_\theta(\mathbf{X})$ as the decoder and encoder neural networks of the VAE, and (θ, ψ) are the weights and biases of

these neural networks. The quantities $f_\psi(\mathbf{Z})$ and $g_\theta(\mathbf{X})$, respectively, output the values of the distributional parameters of $q_\theta(\mathbf{Z}|\mathbf{X})$, i.e. the variational approximation of the true but intractable posterior $p_\psi(\mathbf{Z}|\mathbf{X})$, and $p_\psi(\mathbf{X}|\mathbf{Z})$, i.e. the generative distribution that describes the underlying distribution of the data.

In variational inference, by constraining $q_\theta(\mathbf{Z}|\mathbf{X})$ to be from a class of simple distributions, or a “variational family”, we can obtain the best candidate from within that class of distributions to approximate the true intractable posterior. VAEs also incorporate amortized variational inference (Gershman & Goodman 2014), where the neural network parameters are shared across observations in order to utilize stochastic gradient descent in optimization (Kingma & Welling 2019). In practice, both $q_\theta(\mathbf{Z}|\mathbf{X})$ and $p(\mathbf{Z})$ are typically assumed to have simple forms, such as independent multivariate Gaussians (Kingma & Welling 2013).

The decoder draws samples from the posterior that is learned from the encoder, using the so-called “reparametrization trick” to allow the calculation of gradients through the sampling step (Kingma & Welling 2013). Then, using these samples as input, the decoder outputs the parameters of $p_\psi(\mathbf{X}|\mathbf{Z})$. This decoding process shows how the original data \mathbf{X} is constructed from the latent variable \mathbf{Z} . In this way, the network learns a distribution for \mathbf{Z} , which can be interpreted as a representation of \mathbf{X} in a reduced dimensional space. Also, synthetic data can be generated by sampling from the learned generative model $p_\psi(\mathbf{X}|\mathbf{Z})$, which describes the distribution from which the data originates.

3.1.1 Importance-Weighted Autoencoder

The IWAE (Burda et al. 2015) is a generalization of the standard VAE. Whereas a standard VAE draws one sample from $q_\theta(\mathbf{Z}|\mathbf{X})$, IWAE draws multiple samples, which are used to

create a tighter bound on the marginal log-likelihood than the traditional ELBO (Cremer et al. 2017). The IWAE bound, corresponding to the ELBO in (1), can be written as

$$\mathcal{L}(\theta, \psi) = \mathbb{E}_{\mathbf{z}_1, \dots, \mathbf{z}_K \sim q_\theta(\mathbf{Z}|\mathbf{X})} \log \left[\frac{1}{K} \sum_{k=1}^K \frac{p_\psi(\mathbf{X}|\mathbf{z}_k)p(\mathbf{z}_k)}{q_\theta(\mathbf{z}_k|\mathbf{X})} \right], \quad (2)$$

where K is the number of samples from the posterior. Importantly, Burda et al. (2015) showed that for any $K \geq 1$, $\log p(\mathbf{X}) \geq \mathcal{L}_{K+1} \geq \mathcal{L}_K$, such that $\mathcal{L}_K \rightarrow \log p(\mathbf{X})$ as $K \rightarrow \infty$ if $p_\psi(\mathbf{X}, \mathbf{Z})/q_\theta(\mathbf{Z}|\mathbf{X})$ is bounded. If $K = 1$, (2) reduces to the form of the ELBO in Equation (1), where the IWAE corresponds exactly to the standard VAE. For $K > 1$, the lower bound more closely approximates the true marginal log likelihood, but the computational burden is increased due to the increased number of drawn samples. In this way, the IWAE can be considered to be part of the VAE family, and we refer to methods that use either VAEs or IWAEs broadly as “VAE methods”. A visualization of the workflow for an IWAE (without missing data) can be found in Section 2.1 of the supplementary materials.

3.2 Missing Data

In this section, we introduce notation for missing data and review the different mechanisms of missingness, as described in the statistical literature. Let the data be factored such that $\mathbf{X} = \{\mathbf{X}^o, \mathbf{X}^m\}$, with \mathbf{X}^o denoting the observed values and \mathbf{X}^m denoting the missing values. Also, for each observation vector \mathbf{x}_i , denote \mathbf{x}_i^o and \mathbf{x}_i^m respectively to be the observed and missing features of \mathbf{x}_i , and let \mathbf{R} be a matrix of the same dimensionality as \mathbf{X} , with entries $r_{ij} = I(x_{ij} \text{ is observed})$ for the i^{th} observation and j^{th} feature, where $I(\cdot)$ denotes the indicator function. In this way, \mathbf{R} is the “mask” matrix pertaining to \mathbf{X} , such that $\mathbf{x}_i^o = \{x_{ij} : r_{ij} = 1\}$ and $\mathbf{x}_i^m = \{x_{ij} : r_{ij} = 0\}$ for all $i = 1, \dots, n$ and $j = 1, \dots, p$.

3.2.1 Missingness Mechanisms

Missingness was classified into three major categories, or mechanisms, in the seminal work by Little & Rubin (2002). These mechanisms are missing completely at random (MCAR), missing at random (MAR), and missing not at random (MNAR), and they satisfy the following relations:

- MCAR: $p(\mathbf{r}_i|\mathbf{x}_i, \mathbf{z}_i, \boldsymbol{\phi}) = p(\mathbf{r}_i|\boldsymbol{\phi})$
- MAR: $p(\mathbf{r}_i|\mathbf{x}_i, \mathbf{z}_i, \boldsymbol{\phi}) = p(\mathbf{r}_i|\mathbf{x}_i^o, \boldsymbol{\phi})$
- MNAR: $p(\mathbf{r}_i|\mathbf{x}_i, \mathbf{z}_i, \boldsymbol{\phi}) = p(\mathbf{r}_i|\mathbf{x}_i^o, \mathbf{x}_i^m, \mathbf{z}_i, \boldsymbol{\phi})$

Here, $\boldsymbol{\phi}$ denotes the collection of parameters for the model of the missingness mask $\mathbf{r}_i = \{r_{i1}, \dots, r_{ip}\}$. MCAR missingness is independent of both observed and missing values, and is equivalent to randomly masking a fixed proportion of entries. MAR missingness is dependent on the values of observed entries, but not on any unobserved values, including the missing values themselves.

Importantly, for both MCAR and MAR, the missingness is considered “ignorable” such that the missingness mechanism need not be explicitly modelled in these cases (Rubin 1976, Little & Rubin 2002). In particular, one is often interested in maximizing the quantity $p(\mathbf{X}^o, \mathbf{R})$. Under ignorable missingness, this quantity can be factored as $p(\mathbf{X}^o)p(\mathbf{R}|\mathbf{X}^o)$, where $p(\mathbf{X}^o)$ is the marginal distribution of \mathbf{X}^o . Here, $p(\mathbf{R}|\mathbf{X}^o)$ need not be specified because inference on the parameters of interest pertaining to $p(\mathbf{X}^o)$ is independent of $p(\mathbf{R}|\mathbf{X}^o)$. Then, one aims to maximize the quantity

$$\log p(\mathbf{X}^o) = \log \iint p(\mathbf{X}^o, \mathbf{X}^m, \mathbf{Z})d\mathbf{X}^m d\mathbf{Z} = \log \int p(\mathbf{X}^o, \mathbf{Z})d\mathbf{Z}. \quad (3)$$

Because \mathbf{X}^m can be easily integrated out of (3), this quantity can be bounded below exactly as in Section 3.1, conditioning on just the observed data \mathbf{X}^o , rather than the full data \mathbf{X} . Existing methods typically take advantage of this simplification, and are shown to perform well under ignorable missingness. Details for these methods are given in Section 2.3 of the supplementary materials.

In contrast, MNAR missingness refers to the case where the missingness can be dependent on any unobserved values, including the missing entries \mathbf{x}_i^m . MNAR missingness can also be dependent on \mathbf{x}_i^o as well as latent values like \mathbf{Z} , and thus MNAR represents the most general and difficult case of missingness in practice (Scheffer 2002). In this setting, the missingness is considered “non-ignorable”, and typically requires a model of the missingness \mathbf{r}_i for proper analysis (Stubbendick & Ibrahim 2003, Ibrahim et al. 2005). Variational inference has been used in the presence of MNAR missingness in the past, and has been shown to perform well in the stochastic block model (Tabouy et al. 2019), although it is unclear how to extend this to the VAE family setting. Current methods of the VAE family are only able to handle MAR missingness, and there is no method to properly deal with the more difficult MNAR case. This is compounded by the fact that missingness in EHR datasets has been posited to be non-ignorable (Beaulieu-Jones & and 2016, Venugopalan et al. 2019, Sharafoddini et al. 2019, O’Shea 2019).

Under the MNAR (non-ignorable) missingness assumption, the marginal log-likelihood is written as

$$\log p(\mathbf{X}^o, \mathbf{R}) = \log \iint p(\mathbf{X}^o, \mathbf{X}^m, \mathbf{Z}, \mathbf{R}) d\mathbf{X}^m d\mathbf{Z}. \quad (4)$$

We see here that due to the dependence between \mathbf{R} and \mathbf{X}^m , it is not as straightforward to integrate out the variable pertaining to the missing values \mathbf{X}^m as in (3). A lower bound of this quantity can be derived as before, and variational inference can be performed. We

factorize $p(\mathbf{X}^o, \mathbf{X}^m, \mathbf{Z}, \mathbf{R})$ using the selection model factorization (Diggle & Kenward 1994), which is written as $p(\mathbf{X}^o, \mathbf{X}^m, \mathbf{Z}, \mathbf{R}) = p(\mathbf{X}^o, \mathbf{X}^m | \mathbf{Z})p(\mathbf{Z})p(\mathbf{R} | \mathbf{X}, \mathbf{Z})$.

Now, one needs only to specify a model for the missingness mask $p(\mathbf{R} | \mathbf{X}, \mathbf{Z}, \phi)$. There are a number of ways to specify such a model. For example, Diggle & Kenward (1994) proposes a binomial model for the missing data mechanism:

$$p(\mathbf{R} | \mathbf{X}, \phi) = \prod_{i=1}^n \prod_{j=1}^p [p(r_{ij} = 1 | \mathbf{x}_i, \phi)]^{r_{ij}} [1 - p(r_{ij} = 1 | \mathbf{x}_i, \phi)]^{1-r_{ij}},$$

where $p(r_{ij} = 1 | \mathbf{x}_i, \phi)$ can be modeled straightforwardly by a logistic regression model, such that

$$\text{logit}[p(r_{ij} = 1 | \mathbf{x}_i, \phi)] = \phi_0 + \mathbf{x}_i^o \phi_1 + \mathbf{x}_i^m \phi_2,$$

where $\phi_1 = \{\phi_{11}, \dots, \phi_{1,p_{obs}}\}^T$ and $\phi_2 = \{\phi_{21}, \dots, \phi_{2,p_{miss}}\}^T$ represent the set of coefficients pertaining to the observed features and missing features, respectively, with p_{obs} and p_{miss} denoting the total number of completely-observed and partially-observed features in the data. Note that this model assumes independence of \mathbf{R} across features, such that the missingness of each feature is independent of whether any other feature has been observed, which may or may not be realistic in some settings (Ibrahim et al. 2005). Also, we note that this missingness model does not depend on the latent variable \mathbf{Z} , but such latent factors can also be included as covariates.

Given the high dimensionality of the missingness mask \mathbf{R} and the potential correlation between the mask and the features in EHR data, we take advantage of the deep neural network structure to learn the parameters of the missingness model in Section 3.3. By using an IWAE architecture, we are able to model complex interactions between the features. Also, by appending an additional feed-forward neural network to the decoder, we can jointly learn the conditional distribution $p_\phi(r_{ij} = 1 | \mathbf{x}_i, \mathbf{z}_i, \phi)$ during training of the IWAE,

with ϕ now denoting the weights and biases of this additional neural network, which we call the “mask decoder network”. This provides a simple way to model the dependency of the missingness on the data, while learning complex representations of the data itself. Additionally, we can exactly model the logistic regression model for the missingness mask by omitting hidden layers and using a Sigmoid activation function in the mask decoder network. In this way, the weights associated with the mask decoder network would exactly represent the coefficients of the covariates of the logistic regression model, while the bias represents the intercept. We go over this proposed scheme in more detail in Section 3.3, where we formalize our deep learning architecture to handle MNAR missingness.

In traditional missing data literature with selection model factorization, covariates for the logistic regression model need to be pre-specified based upon prior information. Similarly, we can specify features to include as predictors for our proposed neural network missingness model, such that these features are fed in as input to the mask decoder neural network. Alternatively, when such information is not available, we show that using all features as covariates in the missingness model yields reasonably good performance in most simulated cases, although performance increases when the correct model is specified.

3.3 NIMIWAE: IWAE with Nonignorable Missingness

We now propose a method to perform inference using an IWAE in the presence of missing data whose missingness is nonignorable. First, we specify a general form of the lower bound, and we utilize the general IWAE framework to form a tighter bound on the marginal log-likelihood than the VAE ELBO. Unlike a traditional IWAE, we now have two latent variables \mathbf{Z} and \mathbf{X}^m . Like the traditional IWAE, we draw K samples of \mathbf{Z} , but we additionally draw M samples of \mathbf{X}^m for each sample of \mathbf{Z} in the same manner. The form of the

pertaining lower bound can be derived as follows:

$$\begin{aligned}
\log p(\mathbf{X}^o, \mathbf{R}) &= \log \left[\iint p_{\psi, \phi}(\mathbf{X}^o, \mathbf{X}^m, \mathbf{R}, \mathbf{Z}) d\mathbf{Z} d\mathbf{X}^m \right] \\
&= \sum_{i=1}^n \log \mathbb{E}_{(\mathbf{z}_i, \mathbf{x}_i^m) \sim q_{\theta}(\mathbf{Z}, \mathbf{X}^m)} \left[\frac{p_{\psi, \phi}(\mathbf{x}_i^o, \mathbf{x}_i^m, \mathbf{r}_i, \mathbf{z}_i)}{q_{\theta}(\mathbf{z}_i, \mathbf{x}_i^m)} \right] \\
&\geq \sum_{i=1}^n \mathbb{E}_{(\mathbf{z}_{i1}, \mathbf{x}_{i1}^m), \dots, (\mathbf{z}_{iK}, \mathbf{x}_{iK}^m) \sim q_{\theta}(\mathbf{Z}, \mathbf{X}^m)} \left[\log \frac{1}{K} \sum_{k=1}^K \frac{p_{\psi, \phi}(\mathbf{x}_i^o, \mathbf{x}_{ikl}^m, \mathbf{r}_i, \mathbf{z}_{ik})}{q_{\theta}(\mathbf{z}_{ik}, \mathbf{x}_{ikl}^m)} \right] \quad (5)
\end{aligned}$$

As explained in Section 3.2.1, we use the selection model factorization of the generative model, such that

$$p_{\psi, \phi}(\mathbf{X}^o, \mathbf{X}^m, \mathbf{R}, \mathbf{Z}) = p_{\psi}(\mathbf{X}^o, \mathbf{X}^m | \mathbf{Z}) p(\mathbf{Z}) p_{\phi}(\mathbf{R} | \mathbf{X}^o, \mathbf{X}^m, \mathbf{Z}).$$

Here, ψ denotes the weights and biases of the encoder and decoder neural networks, and ϕ denotes the weights and biases of the mask decoder network that learns the parameters of the missingness model. This is analogous to the standard logistic regression model used in the traditional statistical literature, as given in Section 3.2.1, and is exactly equivalent to the logistic regression model when there are no hidden layers and a Sigmoid activation function is applied to this neural network. With this neural network, more complicated mechanisms of missingness can be explored by incorporating hidden layers and associated activation functions. For the purposes of this study, we leave this as an extension of our method, and focus on the simpler logistic regression model of missingness in our analyses.

Additionally, in MNAR, we must specify a form for the variational approximation $q_{\theta}(\mathbf{Z}, \mathbf{X}^m)$ for the joint posterior, where we treat both \mathbf{Z} and the missing data \mathbf{X}^m as latent variables. This is in contrast to the MAR case, where one only specifies the variational posterior of the latent variable $q_{\theta}(\mathbf{Z})$, and this posterior can be conditioned on just the observed values, such that $q_{\theta}(\mathbf{Z} | \mathbf{X}^o)$. In the MNAR case, we can factor the joint

posterior of $(\mathbf{Z}, \mathbf{X}^m)$ as

$$q_{\theta}(\mathbf{Z}, \mathbf{X}^m) = q_{\theta_1}(\mathbf{Z}|\mathbf{X}^o, \mathbf{R})q_{\theta_2}(\mathbf{X}^m|\mathbf{Z}, \mathbf{X}^o, \mathbf{R}).$$

Applying the factorizations of the generative model and the joint posterior to (5), we obtain the final form of our lower bound, which we call the **NonIgnorably Missing Importance-Weighted AutoEncoder** bound, or “**NIMIWAE** bound”:

$$\sum_{i=1}^n \mathbb{E}_{\{\mathbf{Z}, \mathbf{X}^m\} \sim q_{\theta}(\mathbf{Z}, \mathbf{X}^m)} \left[\log \frac{1}{K} \frac{1}{M} \sum_{k=1}^K \sum_{l=1}^M \frac{p_{\psi}(\mathbf{x}_i|\mathbf{z}_{ik})p(\mathbf{z}_{ik})p_{\phi}(\mathbf{r}_i|\mathbf{x}_i^o, \mathbf{x}_{ikl}^m, \mathbf{z}_{ik})}{q_{\theta_1}(\mathbf{z}_{ik}|\mathbf{x}_i^o, \mathbf{r}_i)q_{\theta_2}(\mathbf{x}_{ikl}^m|\mathbf{z}_{ik}, \mathbf{x}_i^o, \mathbf{r}_i)} \right],$$

where samples of $\{\mathbf{Z}, \mathbf{X}^m\}$ are drawn via ancestral sampling (Bishop 2006), and the entire lower bound is optimized using the Adam optimizer (Kingma & Ba 2014). The NIMI-WAE bound properly accounts for MNAR by the specified mask decoder network for the missingness mechanism \mathbf{r} .

An illustration of this proposed network is given in Figure 1, and the details of the NIMIWAE algorithm are outlined in Section 2.2 of the supplementary materials.

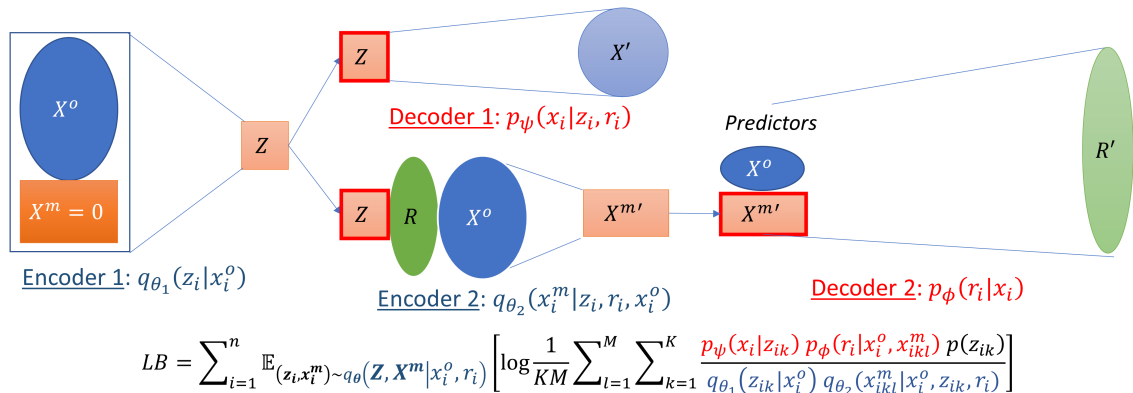


Figure 1: Architecture of proposed NIMIWAE method. Dark colored nodes (X^o , R , $X^m = 0$) represent deterministic values, lightly colored nodes (Z , $X^{m'}$) represent learned distributional parameters, and outlined (in red) nodes represent sampled values. Orange cells correspond to latent variables \mathbf{Z} and \mathbf{X}^m . \mathbf{Z} is sampled K times and \mathbf{X}^m is sampled M times from the respective posteriors. Below is the lower bound (LB), which is optimized via stochastic gradient descent.

4 Simulations

4.1 Simulated Data

Because the true values of missing entries in the Physionet data are unknown, we utilize statistical simulation to first evaluate the imputation performance of our proposed NIMIWAE method under the assumption of MCAR, MAR, and MNAR missingness. We also evaluate the performance of state-of-the-art missing data methods in machine learning that claim to handle up to MAR patterns of missgness: HIVAE (Nazabal et al. 2018), VAEAC (Ivanov et al. 2019), MIWAE (Mattei & Frelsen 2019), MissForest (Stekhoven & Buhlmann 2011),

as well as a naïve mean imputation method. For all simulations and real datasets, we divided the full data into training, validation, and test datasets with ratio 6:2:2. Each model was trained on the training set, and hyperparameters were validated using the validation set. The test set is held out in the training and hyperparameter tuning, and final imputation performance was evaluated on just the test set, ensuring that there is no overfitting in the model. For MissForest and mean imputation, we impute only the test dataset, for consistency across all methods. For NIMIWAE, we utilize all features in the missingness model unless otherwise specified.

The simulated data \mathbf{X} is an $n \times p$ matrix with $n = 100,000$ observations and $p = 100$ features, and the latent dimensionality was $d = 2$. This data was obtained by using a linear transformation of the latent values: $\mathbf{X} = \mathbf{Z}\mathbf{W} + \mathbf{B}$, where \mathbf{W} and \mathbf{B} were both drawn from $N(0, 1)$ and are matrices of dimensions $d \times p$ and $n \times p$, respectively, and \mathbf{Z} was drawn from $N_{100}(\mathbf{0}, \mathbf{I})$. We then simulated the missingness mask \mathbf{R} on half of the simulated features by using a logistic regression model, such that $\text{logit}[p(r_{ij_m} = 1 | \mathbf{X}, \boldsymbol{\phi})] = \phi_0 + \boldsymbol{\phi}_1 \mathbf{X}^o + \boldsymbol{\phi}_2 \mathbf{X}^m$, where $j'_m = 1, \dots, p_{miss}$ index the missing features and $j_o = 1, \dots, p_{obs}$ index the observed features, $\boldsymbol{\phi}_2 = \{\phi_{21}, \dots, \phi_{2,p_{miss}}\}$ are those pertaining to the missing features, and $\boldsymbol{\phi}_1 = \{\phi_{11}, \dots, \phi_{1,p_{obs}}\}$ are the coefficients pertaining to the observed features, where p_{obs} and p_{miss} are the total number of features that are observed and missing, respectively, with $p_{obs} = p_{miss} = p/2$. We draw nonzero values of $\boldsymbol{\phi}_1$ and $\boldsymbol{\phi}_2$ from the log-normal distribution with mean $\mu = 5$ and log standard deviation $\sigma = 0.2$.

Then, each missingness mechanism was simulated as follows: 1) MCAR missingness: $\{\boldsymbol{\phi}_1, \boldsymbol{\phi}_2\} = 0$, 2) MAR missingness: $\boldsymbol{\phi}_2 = 0$ and one of $\boldsymbol{\phi}_1 \neq 0$, and 3) MNAR missingness: $\boldsymbol{\phi}_1 = 0$, and one of $\boldsymbol{\phi}_2 \neq 0$. For MAR and MNAR, we use just one feature as a covariate for the missingness model for each missing feature. Specifically, for MAR, we pair each missing

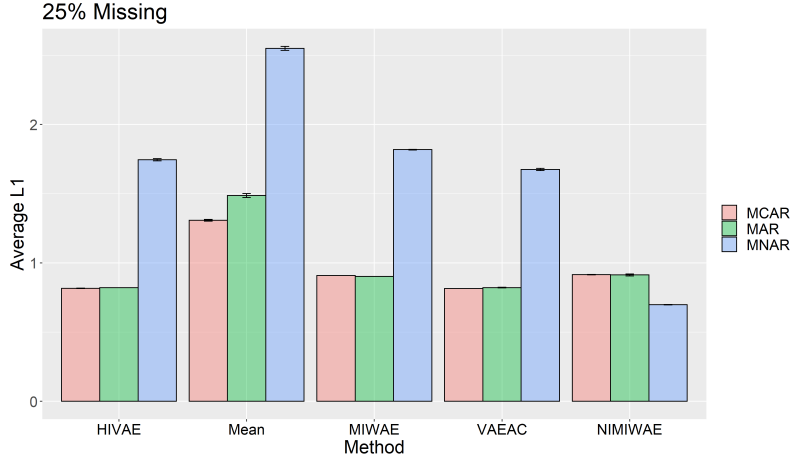


Figure 2: Average L1 distance between true and imputed values for missing entries, stratified by simulated mechanism of missingness. Again, NIMIWAE outperforms all methods in imputing missing values that were simulated to be MNAR.

feature $j_m = 1, \dots, p_{miss}$ with a unique observed feature $j_o = 1, \dots, p_{obs}$, which contains no missingness, and use the paired observed feature as the covariate. For MNAR, we use each missing feature j_m itself as the only covariate in its respective missingness model. In this way, for each MAR or MNAR features, the missingness is dependent on just one feature.

We measured imputation performance for by calculating the average L1 distance between true and imputed masked values. Results were averaged over 5 simulated datasets per simulation condition, spanning various missingness mechanisms and percent missingness. Letting $\hat{\mathbf{X}}^m$ denote the imputed masked values of the true \mathbf{X}^m values of the missing entries, the average L1 distance is simply

$$\frac{|\hat{\mathbf{X}}^m - \mathbf{X}^m|}{N_{miss}},$$

where N_{miss} is the total number of missing entries in the dataset.

Figure 2 shows the average L1 distance yielded by each method, stratified by the simulated mechanism of missingness. We note that for each these simulations, we utilize all features in NIMIWAE’s mask decoder network, although only one feature is involved under the true missingness model. Despite this, NIMIWAE consistently yields drastically greater performance compared to other methods under MNAR missingness, while yielding an average L1 that is comparable to other MAR methods in the MCAR and MAR cases. This demonstrates that the neural network is able to learn the correct underlying missingness model under MNAR despite overspecification. This can be exceptionally useful for real EHR data, where the true covariates of the missingness model under MNAR may not be known a priori.

One may also be interested in the performance of these missing data methods in lower-dimensional data. Thus, we simulated datasets of smaller dimensions ($p = 8$), and similarly imputed each dataset. Results of this analysis can be found in Section 2.4 of the supplementary materials. Details and values of the hyperparameters that were searched for all datasets, including these simulated datasets, can be found in Section 2.5 of the supplementary materials.

4.2 UCI Datasets

Next, we performed imputation of simulated missing entries on several real datasets from the UCI Machine Learning repository (Dua & Graff 2017) to evaluate NIMIWAE’s performance in other real-life datasets with potentially complex feature interactions like in the Physionet data. We simulated MCAR, MAR, and MNAR missingness on these datasets using the same logistic regression model as in the prior simulation, with a fixed 25% of the overall entries missing. MissForest was not able to be run on two of the UCI datasets (hep-

mass, power) due to memory issues. Table 2 shows imputation performance of each method on each dataset, with masks simulated based on MCAR, MAR, and MNAR missingness.

We found that NIMIWAE consistently performs well when the missingness is simulated to be MNAR. In practice, explicitly modeling the missingness model may be problematic in smaller datasets, as a model that is too large tends to significantly hinder performance for MNAR methods when the true mechanism is MAR or MCAR (Ibrahim et al. 2005). As a result, we see that for some datasets, NIMIWAE yields poorer imputation performance (high average L1) compared to other methods when the missingness is ignorable. We found that when the mask decoder network was omitted, the imputation performance by NIMIWAE generally improved under MCAR and MAR missingness, and was similar to the performance of state-of-the-art methods. We denote this NIMIWAE framework without the mask decoder network “Ignorably-Missing IWAE” (IMIWAE). This highlights the importance of the assumption of ignorability of the missingness, especially in datasets of smaller size. Typically in the statistical literature, an a priori assumption is made on whether the missingness in the data is ignorable or non-ignorable. Generally, NIMIWAE allows excellent performance without such an assumption, but IMIWAE may be more appropriate for small datasets where ignorable missingness is suspected.

5 Physionet 2012 Challenge Dataset

Finally, we analyzed the Physionet 2012 Challenge data using each of the compared methods. Namely, we perform a qualitative analysis of each imputed dataset, highlighting differences between results from assuming non-ignorable (NIMIWAE) and ignorable (IMIWAE) missingness (Ibrahim et al. 2005, Ibrahim & Molenberghs 2009). This is because, in con-

trast to our simulations, the true values of the missing entries are not available to directly assess imputation performance, and it may be infeasible to simulate additional missing entries by masking observed values in real data due to a high rate of inherent missingness in the data. Additionally, the missingness mechanism itself is generally not “testable” by the observed data in practice (Ibrahim et al. 1999). Similar to the simulations, we evaluate the imputation results from state-of-the-art methods as well.

Blood pressure has often been used as a measure of risk for patients, with associations found between abnormal diastolic, systolic blood pressure (DBP, SBP), and mean arterial pressure (MAP) and mortality in adults admitted into the ICU (Maheshwari et al. 2018, Burstein et al. 2020). In the Physionet dataset, we found that the rates of missingness for invasive DBP, SBP, and MAP measurements were higher for patients who survived the ICU stay than for those who did not. One possible explanation for this is that these tests may not be performed as routinely for a patient that is not in critical condition, thus yielding a higher rate of missingness if the patient is in better cardiovascular health. This may suggest MNAR missingness, where we may expect the missing blood pressure measurements to be closer to “normal” range relative to the observed values. The accepted “normal” or healthy values of SBP and DBP are under 120 and 80, respectively (Robinson 1939), while the “normal” range of MAP is between 65 to 100 (Jakkula et al. 2018).

We imputed missing values for blood pressure measurements using each of the compared methods, and Figure 3 shows the distribution of the imputed values from these methods, as well as the rate of missingness for each measurement with respect to the mortality status of each patient. We found that the rates of missingness for these measurements were on average about 2% higher for patients who survived the ICU stay than those who did not survive. Also, we found that the imputed DBP and SBP were significantly lower

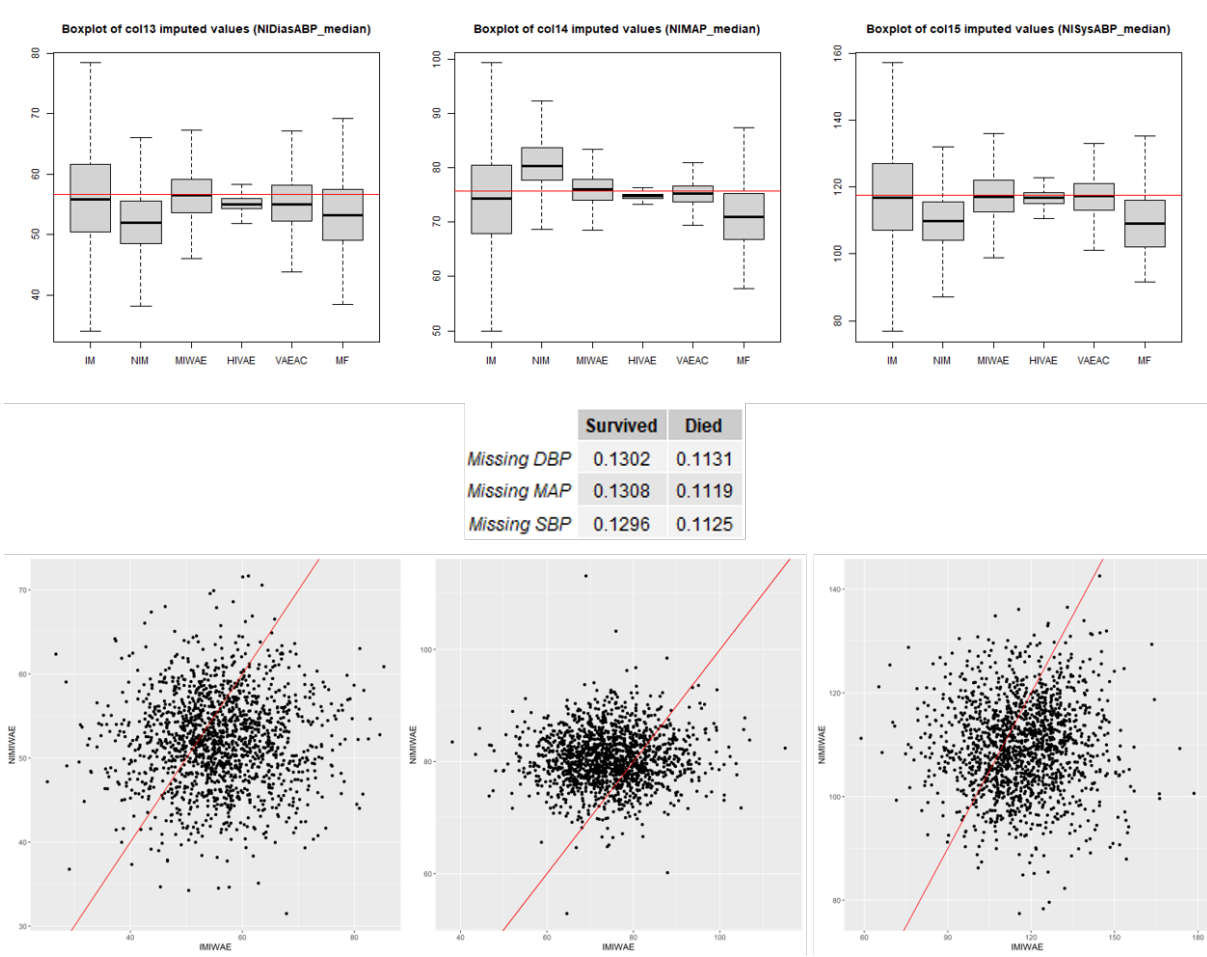


Figure 3: (Top 3): Boxplots of imputed values via IMIWAE (IM), NIMIWAE (NIM), MIWAE, HIVAE, VAEAC, and MissForest (MF) of imputation for median DBP (left), MAP (center), and SBP (right). Mean imputed values are given with the horizontal red line. (Middle): Table of missingness rates for median DBP, MAP, and SBP, stratified by whether each patient survived the ICU stay. (Bottom 3): Scatterplots of NIMIWAE imputed values vs. IMIWAE imputed values, showing the shift in values when using a non-ignorably missing model vs. an ignorably missing model. The $y = x$ line is given in red.

for NIMIWAE and MissForest than all other methods, suggesting better health of the patients who had missingness in these measurements. Furthermore, MAP values imputed by NIMIWAE was most consistent with the normal or “healthy” range of MAP values than other methods, with 99.6% of measurements within the “normal” range. This is in line with the missingness pattern, which showed a lower rate of mortality for patients with missingness in these blood pressure measurements.

Based on the imputed datasets from these methods, we also fit a logistic regression model with mortality as the response, with the features of this dataset as the covariates. We report details of the covariates with the top 5 largest effects on mortality when using the imputed dataset from the non-ignorably missing NIMIWAE model in Table 3. We found some significant differences in the results of the logistic regression based on the different imputed datasets. For example, we found that for “MechVentLast8Hour”, the Z statistic was significantly higher with NIMIWAE than with any other model, suggesting that the NIMIWAE-imputed dataset found this feature to be more significant in modelling the mortality than other imputed datasets. Another observation we made was that whereas imputed values from the ignorable version of our model (IMIWAE) found “FiO2_last” and “pH_last” to be insignificant to mortality, NIMIWAE found these features to be highly significant, with Z-statistic values of 4.83 and 3.41, respectively. Clinical studies have shown that irregular levels of FiO2 and pH may be significant predictors of mortality in hospital patients (Samanta et al. 2018, von Vopelius-Feldt et al. 2020), and the dataset imputed by the non-ignorable model better captures these effects.

6 Discussion

In this paper we introduce NIMIWAE, one of the first methods to handle up to MNAR patterns of missingness in the VAE/IWAE class of methods, to address complex patterns of missingness observed in the Physionet EHR data. Using statistical simulations, we show that NIMIWAE performs well in imputing missing features under MNAR, and has reasonable performance under the MCAR or MAR settings. Performance in imputing MCAR and MAR missingness can be further improved in NIMIWAE by using the ignorable version of this model (IMIWAE), where we omit the mask decoder network. We also found that the results of the analysis on the Physionet data are highly dependent on the choice of missingness model, which specifies the assumption of the missingness mechanism. However, NIMIWAE is able to impute missing values well in simulations regardless of the underlying missingness mechanism, flexibly modelling the mechanism using a deeply-learned neural network. We have also shown that this performance can be further improved if a priori knowledge is used to narrow down the missingness model covariates, while the neural network structure allows this model to capture complex, nonlinear dependencies between missingness across features. The NIMIWAE-imputed dataset resulted in more realistic imputed values with respect to what we may expect in the Physionet Challenge patients, since NIMIWAE takes into account possible non-ignorable missingness in the data. Additionally, the IWAE architecture learns a lower-dimensional representation of the data, which can be used for further tasks, such as patient subgroup identification or visualization of data.

Learning algorithms that can be applied to EHR data like the Physionet Challenge dataset can be valuable tools that clinicians can use to aid decisions in hospital settings and understand patterns within these health records. For example, properly handling missingness in EHRs when imputing the missing entries can improve the performance of

prediction algorithms that can assess risk of death or other outcomes of interest, like disease. Informative missingness is a common problem in analyzing EHR data, and accounting for such missingness can be helpful in obtaining accurate, unbiased estimates of the true missing values. We note that although we have used our NIMIWAE method primarily to analyze the Physionet 2012 Challenge dataset, it can more generally be applied to settings where one wishes to train a VAE when missingness is present among input features.

SUPPLEMENTARY MATERIAL

Supplementary Materials: Descriptions of real datasets used, directions on how to obtain datasets, and link to code for reproducibility. (pdf)

R-package for NIMIWAE routine: R-package NIMIWAE containing code to perform the diagnostic methods described in the article. The package can be downloaded from <https://github.com/DavidKLim/NIMIWAE> (website)

R Paper repo for reproducibility: Github repository to replicate all analyses, figures, and tables from this paper can be found here: https://github.com/DavidKLim/NIMIWAE_Paper (website)

Acknowledgments

This research was supported by NIH grant 5T32CA106209-13.

References

- Beaulieu-Jones, B. K. & and, J. H. M. (2016), Missing Data Imputation in the Electronic Health Record Using Deeply Learned Autoencoders, *in* ‘Biocomputing 2017’, WORLD SCIENTIFIC.
- Beesley, L. J. & Mukherjee, B. (2020), ‘Statistical inference for association studies using electronic health records: handling both selection bias and outcome misclassification’, *Biometrics* .
URL: <https://onlinelibrary.wiley.com/doi/abs/10.1111/biom.13400>
- Bishop, C. M. (2006), *Pattern Recognition and Machine Learning*, Springer-Verlag New York Inc.
- Blei, D. M., Kucukelbir, A. & McAuliffe, J. D. (2016), ‘Variational Inference: A Review for Statisticians’, *arXiv e-prints* p. arXiv:1601.00670.
- Burda, Y., Grosse, R. & Salakhutdinov, R. (2015), ‘Importance Weighted Autoencoders’, *arXiv e-prints* p. arXiv:1509.00519.
- Burstein, B., Tabi, M., Barsness, G. W., Bell, M. R., Kashani, K. & Jentzer, J. C. (2020), ‘Association between mean arterial pressure during the first 24 hours and hospital mortality in patients with cardiogenic shock’, *Critical Care* **24**(1).
- Citi, L. & Barbieri, R. (2012), Physionet 2012 challenge: Predicting mortality of icu patients using a cascaded svm-glm paradigm, *in* ‘2012 Computing in Cardiology’, pp. 257–260.
- Courtright, K. R., Chivers, C., Becker, M., Regli, S. H., Pepper, L. C., Draugelis, M. E. & O’Connor, N. R. (2019), ‘Electronic health record mortality prediction model for targeted

- palliative care among hospitalized medical patients: a pilot quasi-experimental study’, *Journal of General Internal Medicine* **34**(9), 1841–1847.
- Cremer, C., Morris, Q. & Duvenaud, D. (2017), ‘Reinterpreting Importance-Weighted Autoencoders’, *arXiv e-prints* p. arXiv:1704.02916.
- Diggle, P. & Kenward, M. G. (1994), ‘Informative drop-out in longitudinal data analysis’, *Applied Statistics* **43**(1), 49.
- Doersch, C. (2016), ‘Tutorial on Variational Autoencoders’, *arXiv e-prints* p. arXiv:1606.05908.
- Dua, D. & Graff, C. (2017), ‘UCI machine learning repository’.
URL: <http://archive.ics.uci.edu/ml>
- Ferreira, F. L. (2001), ‘Serial evaluation of the SOFA score to predict outcome in critically ill patients’, *JAMA* **286**(14), 1754.
- Fortuin, V., Baranchuk, D., Rätsch, G. & Mandt, S. (2019), ‘Gp-vae: Deep probabilistic time series imputation’.
- Gall, J.-R. L., Loirat, P., Alperovitch, A., Glaser, P., Granthil, C., Mathieu, D., Mercier, P., Thomas, R. & Villers, D. (1984), ‘A simplified acute physiology score for ICU patients’, *Critical Care Medicine* **12**(11), 975–977.
- Gershman, S. J. & Goodman, N. D. (2014), Amortized inference in probabilistic reasoning, *in* ‘CogSci’.
- Ghosh, P., Sajjadi, M. S. M., Vergari, A., Black, M. & Schölkopf, B. (2019), ‘From Variational to Deterministic Autoencoders’, *arXiv e-prints* p. arXiv:1903.12436.

- Gootjes-Dreesbach, L., Sood, M., Sahay, A., Hofmann-Apitius, M. & Fröhlich, H. (2019), ‘Variational autoencoder modular bayesian networks (VAMBN) for simulation of heterogeneous clinical study data’.
- Ibrahim, J. G., Chen, M.-H., Lipsitz, S. R. & Herring, A. H. (2005), ‘Missing-data methods for generalized linear models’, *Journal of the American Statistical Association* **100**(469), 332–346.
- Ibrahim, J. G., Lipsitz, S. R. & Chen, M.-H. (1999), ‘Missing covariates in generalized linear models when the missing data mechanism is non-ignorable’, *Journal of the Royal Statistical Society: Series B (Statistical Methodology)* **61**(1), 173–190.
- Ibrahim, J. G. & Molenberghs, G. (2009), ‘Missing data methods in longitudinal studies: a review’, *TEST* **18**(1), 1–43.
- Ivanov, O., Figurnov, M. & Vetrov, D. (2019), Variational autoencoder with arbitrary conditioning, in ‘International Conference on Learning Representations’.
URL: <https://openreview.net/forum?id=SyxtJh0qYm>
- Jakkula, P., , Pettilä, V., Skrifvars, M. B., Hästbacka, J., Loisa, P., Tiainen, M., Wilkman, E., Toppila, J., Koskue, T., Bendel, S., Birkelund, T., Laru-Sompa, R., Valkonen, M. & Reinikainen, M. (2018), ‘Targeting low-normal or high-normal mean arterial pressure after cardiac arrest and resuscitation: a randomised pilot trial’, *Intensive Care Medicine* **44**(12), 2091–2101.
- Johnson, A. E., Kramer, A. A. & Clifford, G. D. (2014), Data preprocessing and mortality prediction: The physionet/cinc 2012 challenge revisited, in ‘Computing in Cardiology 2014’, pp. 157–160.

- Johnson, A. E. W., Dunkley, N., Mayaud, L., Tsanas, A., Kramer, A. A. & Clifford, G. D. (2012), Patient specific predictions in the intensive care unit using a bayesian ensemble, *in* ‘2012 Computing in Cardiology’, pp. 249–252.
- Kingma, D. P. & Ba, J. (2014), ‘Adam: A Method for Stochastic Optimization’, *arXiv e-prints* p. arXiv:1412.6980.
- Kingma, D. P. & Welling, M. (2013), ‘Auto-Encoding Variational Bayes’, *arXiv e-prints* p. arXiv:1312.6114.
- Kingma, D. P. & Welling, M. (2019), ‘An Introduction to Variational Autoencoders’, *arXiv e-prints* p. arXiv:1906.02691.
- LeCun, Y., Bengio, Y. & Hinton, G. (2015), ‘Deep learning’, *Nature* **521**(7553), 436–444.
- Little, R. J. A. & Rubin, D. B. (2002), *Statistical Analysis with Missing Data*, John Wiley & Sons, Inc.
- Luo, Y., Cai, X., ZHANG, Y., Xu, J. & xiaojie, Y. (2018), Multivariate time series imputation with generative adversarial networks, *in* S. Bengio, H. Wallach, H. Larochelle, K. Grauman, N. Cesa-Bianchi & R. Garnett, eds, ‘Advances in Neural Information Processing Systems 31’, Curran Associates, Inc., pp. 1596–1607.
- URL:** <http://papers.nips.cc/paper/7432-multivariate-time-series-imputation-with-generative-adversarial-networks.pdf>
- Maheshwari, K., Nathanson, B. H., Munson, S. H., Khangulov, V., Stevens, M., Badani, H., Khanna, A. K. & Sessler, D. I. (2018), ‘The relationship between ICU hypotension and in-hospital mortality and morbidity in septic patients’, *Intensive Care Medicine* **44**(6), 857–867.

- Mattei, P.-A. & Frelsen, J. (2019), MIWAE: Deep generative modelling and imputation of incomplete data sets, *in* K. Chaudhuri & R. Salakhutdinov, eds, ‘Proceedings of the 36th International Conference on Machine Learning’, Vol. 97 of *Proceedings of Machine Learning Research*, PMLR, Long Beach, California, USA, pp. 4413–4423.
URL: <http://proceedings.mlr.press/v97/mattei19a.html>
- Nazabal, A., Olmos, P. M., Ghahramani, Z. & Valera, I. (2018), ‘Handling Incomplete Heterogeneous Data using VAEs’, *arXiv e-prints* p. arXiv:1807.03653.
- O’Shea, R. (2019), ‘Interpreting Missing Data Patterns in the ICU’, *arXiv e-prints* p. arXiv:1912.08612.
- Rezende, D. J., Mohamed, S. & Wierstra, D. (2014), ‘Stochastic Backpropagation and Approximate Inference in Deep Generative Models’, *arXiv e-prints* p. arXiv:1401.4082.
- Robinson, S. C. (1939), ‘Range of normal blood pressure’, *Archives of Internal Medicine* **64**(3), 409.
- Ross, M. K., Wei, W. & Ohno-Machado, L. (2014), ‘“big data” and the electronic health record’, *Yearbook of Medical Informatics* **23**(01), 97–104.
- Rubin, D. B. (1976), ‘Inference and missing data’, *Biometrika* **63**(3), 581–592.
- Sadati, N., Zafar Nezhad, M., Babu Chinnam, R. & Zhu, D. (2019), ‘Representation Learning with Autoencoders for Electronic Health Records: A Comparative Study’, *arXiv e-prints* p. arXiv:1908.09174.
- Samanta, S., Singh, R. K., Baronia, A. K., Mishra, P., Poddar, B., Azim, A. & Gurjar, M. (2018), ‘Early ph change predicts intensive care unit mortality.’, *Indian journal of*

critical care medicine : peer-reviewed, official publication of Indian Society of Critical Care Medicine **22**, 697–705.

Scheffer, J. (2002), ‘Dealing with missing data’, *Research Letters in the Information and Mathematical Sciences* **3**(1), 153–160.

Sharafoddini, A., Dubin, J. A., Maslove, D. M. & Lee, J. (2019), ‘A new insight into missing data in intensive care unit patient profiles: Observational study’, *JMIR Medical Informatics* **7**(1), e11605.

Shickel, B., Tighe, P. J., Bihorac, A. & Rashidi, P. (2018), ‘Deep EHR: A survey of recent advances in deep learning techniques for electronic health record (EHR) analysis’, *IEEE Journal of Biomedical and Health Informatics* **22**(5), 1589–1604.

Silva, I., Moody, G., Scott, D. J., Celi, L. A. & Mark, R. G. (2012), ‘Predicting in-hospital mortality of icu patients: The physionet/computing in cardiology challenge 2012.’, *Computing in cardiology* **39**, 245–248.

Stekhoven, D. J. & Buhlmann, P. (2011), ‘MissForest–non-parametric missing value imputation for mixed-type data’, *Bioinformatics* **28**(1), 112–118.

Stubbendick, A. L. & Ibrahim, J. G. (2003), ‘Maximum likelihood methods for nonignorable missing responses and covariates in random effects models’, *Biometrics* **59**(4), 1140–1150.

Tabouy, T., Barbillon, P. & Chiquet, J. (2019), ‘Variational inference for stochastic block models from sampled data’, *Journal of the American Statistical Association* pp. 1–23.

Tschannen, M., Bachem, O. & Lucic, M. (2018), ‘Recent Advances in Autoencoder-Based Representation Learning’, *arXiv e-prints* p. arXiv:1812.05069.

- van den Oord, A., Vinyals, O. & kavukcuoglu, k. (2017), Neural discrete representation learning, *in* I. Guyon, U. V. Luxburg, S. Bengio, H. Wallach, R. Fergus, S. Vishwanathan & R. Garnett, eds, ‘Advances in Neural Information Processing Systems’, Vol. 30, Curran Associates, Inc., pp. 6306–6315.
- URL:** <https://proceedings.neurips.cc/paper/2017/file/7a98af17e63a0ac09ce2e96d03992fbc-Paper.pdf>
- Venugopalan, J., Chanani, N., Maher, K. & Wang, M. D. (2019), ‘Novel data imputation for multiple types of missing data in intensive care units’, *IEEE Journal of Biomedical and Health Informatics* **23**(3), 1243–1250.
- Vinzamuri, B. & Reddy, C. K. (2013), Cox regression with correlation based regularization for electronic health records, *in* ‘2013 IEEE 13th International Conference on Data Mining’, pp. 757–766.
- von Vopelius-Feldt, J., Watson, D., Swanson-Low, C. & Cameron, J. (2020), ‘Estimated spO₂/fio₂ ratio to predict mortality in patients with suspected COVID-19 in the emergency department: a prospective cohort study’.
- Wang, Y., Yao, H. & Zhao, S. (2016), ‘Auto-encoder based dimensionality reduction’, *Neurocomputing* **184**, 232–242.
- Wells, B. J., Nowacki, A. S., Chagin, K. & Kattan, M. W. (2013), ‘Strategies for handling missing data in electronic health record derived data’, *eGEMs (Generating Evidence & Methods to improve patient outcomes)* **1**(3), 7.
- Zhang, G., Beesley, L. J., Mukherjee, B. & Shi, X. (2020), ‘Patient recruitment using

electronic health records under selection bias: a two-phase sampling framework', *arXiv preprint arXiv:2011.06663* .

	Feature	Missingness (overall)	Patients with ≥ 1 obs.
1	ALP	0.984	0.425
2	ALT	0.983	0.434
3	AST	0.983	0.434
4	Albumin	0.987	0.406
5	BUN	0.928	0.986
6	Bilirubin	0.983	0.435
7	Cholesterol	0.998	0.079
8	Creatinine	0.927	0.986
9	DiasABP	0.458	0.703
10	FiO2	0.843	0.677
11	GCS	0.680	0.986
12	Glucose	0.932	0.976
13	HCO3	0.929	0.984
14	HCT	0.905	0.985
15	HR	0.098	0.986
16	K	0.924	0.980
17	Lactate	0.959	0.548
18	MAP	0.461	0.701
19	Mg	0.929	0.977
20	MechVent	0.849	0.632
21	NIDiasABP	0.579	0.875
22	NIMAP	0.585	0.873
23	NISysABP	0.579	0.877
24	Na	0.929	0.983
25	PaCO2	0.885	0.755
26	PaO2	0.885	0.755
27	Platelets	0.926	0.984
28	RespRate	0.759	0.278
29	SaO2	0.960	0.448
30	SysABP	0.458	0.703
31	Temp	0.629	0.986
32	TroponinI	0.998	0.047
33	TroponinT	0.989	0.220
34	Urine	0.307	0.975
35	WBC	0.933	0.983
36	pH	0.879	0.760

Table 1: Proportion of overall missingness, and proportion of patients with at least 1 measurement for each feature in the Physionet 2012 Challenge EHR dataset.

Dataset		HIVAE	Mean	MissForest	MIWAE	VAEAC	NIMIWAE	IMIWAE
banknote	<i>MCAR</i>	1.50	2.00	1.04	1.46	1.31	1.45	1.31
	<i>MAR</i>	2.14	2.23	1.96	2.89	1.76	5.02	2.41
	<i>MNAR</i>	3.25	3.90	3.37	3.21	3.45	1.75	3.33
concrete	<i>MCAR</i>	44.88	50.30	34.79	40.59	32.15	40.54	35.47
	<i>MAR</i>	63.20	58.64	61.56	60.39	58.36	63.64	57.60
	<i>MNAR</i>	60.77	103.50	90.13	70.57	68.03	55.20	66.24
hepmass	<i>MCAR</i>	0.75	0.82	NA	0.81	0.67	0.83	0.81
	<i>MAR</i>	0.76	0.84	NA	0.86	0.70	1.38	0.85
	<i>MNAR</i>	1.41	1.54	NA	1.37	1.36	0.76	1.37
power	<i>MCAR</i>	0.53	0.72	NA	0.68	0.52	0.90	0.84
	<i>MAR</i>	0.64	0.81	NA	0.82	0.60	0.84	0.82
	<i>MNAR</i>	1.05	1.08	NA	1.07	1.09	1.00	1.02
red	<i>MCAR</i>	1.07	1.41	0.89	1.04	0.96	1.29	1.09
	<i>MAR</i>	1.31	1.69	1.21	1.32	1.31	1.52	1.46
	<i>MNAR</i>	2.00	3.02	2.10	1.73	2.33	1.00	1.68
white	<i>MCAR</i>	2.26	2.62	1.93	2.56	1.97	2.19	2.19
	<i>MAR</i>	2.17	2.63	1.96	2.34	1.95	2.41	2.19
	<i>MNAR</i>	4.10	4.92	3.97	4.49	4.09	3.10	4.67

Table 2: Average L1 distance between true and imputed missing values in various datasets, under different mechanisms of simulated missingness. Proportion of missing entries was fixed at 50%. For NIMIWAE, we additionally ran the “Ignorable” model with the mask decoder network omitted (IMIWAE). We see that NIMIWAE consistently performs relatively well in imputing MNAR missingness, while performance of the “Ignorable” IMIWAE model is comparable to other methods under MCAR and MAR.

Effect	Method	Estimate	SE	Z-stat	p value	95% Interval
FiO2_last	IMIWAE	0	0	-0.891	0.37	(-0.01,0)
	NIMIWAE	1.13	0.23	4.834	0	(0.67,1.58)
	HIVAE	1.08	0.26	4.087	0	(0.56,1.59)
	VAEAC	0.6	0.29	2.098	0.04	(0.04,1.16)
	Mean	1.16	0.26	4.44	0	(0.65,1.68)
	MF	0.86	0.26	3.283	0	(0.35,1.38)
Lactate_last	IMIWAE	0.16	0.03	6.201	0	(0.11,0.21)
	NIMIWAE	0.19	0.03	6.616	0	(0.13,0.24)
	HIVAE	0.21	0.03	6.882	0	(0.15,0.27)
	VAEAC	0.19	0.03	6.015	0	(0.13,0.26)
	Mean	0.23	0.03	6.811	0	(0.16,0.29)
	MF	0.21	0.03	6.32	0	(0.14,0.27)
Mg_last	IMIWAE	0.12	0.08	1.503	0.13	(-0.04,0.28)
	NIMIWAE	0.21	0.12	1.729	0.08	(-0.03,0.45)
	HIVAE	0.23	0.13	1.795	0.07	(-0.02,0.48)
	VAEAC	0.26	0.13	2.064	0.04	(0.01,0.51)
	Mean	0.3	0.13	2.265	0.02	(0.04,0.55)
	MF	0.25	0.13	1.92	0.05	(-0.01,0.51)
pH_last	IMIWAE	0	0	-1.321	0.19	(-0.01,0)
	NIMIWAE	1.18	0.37	3.211	0	(0.46,1.89)
	HIVAE	1.36	0.39	3.481	0	(0.59,2.12)
	VAEAC	1.04	0.37	2.825	0	(0.32,1.77)
	Mean	1.07	0.39	2.746	0.01	(0.31,1.84)
	MF	1.29	0.39	3.352	0	(0.54,2.05)
MechVentLast8Hour	IMIWAE	0.42	0.12	3.411	0	(0.18,0.66)
	NIMIWAE	0.31	0.09	3.413	0	(0.13,0.49)
	HIVAE	0.24	0.19	1.301	0.19	(-0.12,0.61)
	VAEAC	0.4	0.25	1.605	0.11	(-0.09,0.9)
	Mean	0.74	0.28	2.654	0.01	(0.19,1.29)
	MF	0.5	0.22	2.324	0.02	(0.08,0.92)

Table 3: Table of coefficient estimates, standard errors (SE), Z statistics, p-values, and 95% confidence intervals of select covariates from a logistic regression model fit with datasets with missing entries imputed by each method. Here, IMIWAE is the ignorable version of NIMIWAE.